Evidence of longitudinal resonance and optical sub-surface phonons in Al(001)

Vasile Chis and Bo Hellsing

Physics Department, Göteborgs University, Fysikgränd 3, S-412 96 Göteborg, Sweden

E-mail: Vasile.Chis@physics.gu.se

Giorgio Benedek and Marco Bernasconi

Dipartimento di Scienza dei Materiali, Università di Milano-Bicocca, Via Cozzi 53, 20125 Milano, Italy

J. P. Toennies

Max-Planck-Institut für Dynamik und Selbstorganization, Bunsenstrasse 10, 37072 Göttingen, Germany

Abstract.

A calculation of the surface phonon dispersion curves of Al(001) based on the density functional perturbation theory confirms the intrinsic nature of the controversial longitudinal surface phonon resonance, which has been reported to occur in most metal surfaces. The results support previous density-response pseudopotential and semi-empirical Born-von-Kàrmàn calculations by Franchini, Bortolani, *et. al.*, proving the extended nature of the surface perturbation. The latter implies the existence of a Lucas pair of optical surface modes localized in the second layer.

1. Introduction

Many important properties of metal surfaces, such as the relaxation of the surface atomic layers and the surface-dependent work function, are determined by the redistribution of the surface electronic charge with respect to the charge density in the bulk [1, 2]. Another feature, apparently common to most metal surfaces, is the longitudinal (L) surface phonon resonance, which was first discovered by means of inelastic Helium atom spectroscopy (HAS) in silver [3] and other noble metals [4], and subsequently in practically all investigated simple and transition metals [5]. Most of these observations have been confirmed by Electron energy loss spectroscopy (EELS) [5]. This ubiquitous acoustic resonance invariably occurs well below the edge of the longitudinally polarized bulk band, even for the densely packed (111) surface of fcc metals, where no surface longitudinal mode is expected for an ideal surface with simple nearest-neighbor force constants [6]. For this reason this new surface mode was frequently referred to as anomalous longitudinal resonance. The above observations led to considerable theoretical activity in search of a simple explanation. A thorough discussion of the *ab-initio* studies devoted to the surface dynamics of metals, with a comparison to former semi-empirical approaches, can be found in a review by Heid and Bohnen [7].

Whereas HAS and EELS spectroscopies are in agreement as regard the location of the L resonance, there is however a substantial difference between the respective scattering amplitudes, the HAS intensity for the L resonance being often much larger than that for the Rayleigh wave (RW) [3, 4, 5], whereas the EELS amplitude for the L mode is normally much smaller [7, 8]. This was regarded as a paradox since electrons in the inelastic impact regime are essentially scattered by the oscillation of the atom cores of the first two or three surface layers, whereas He atoms are scattered by the oscillations of the surface electron density about 2-3 Å away from the first atomic layer and should be rather insensitive to the atomic displacements parallel to the surface. For these facts Heid and Bohnen [7] conjectured that the L resonance may be attributed to some special property, if not an artifact, of the He-surface interaction and not to a real spectral feature of metal surface dynamics.

This rather unsatisfactory explanation for an apparently universal property of metal surfaces motivated the present study of the surface phonon dispersion curves of Al(001) based on Density functional perturbation theory (DFPT) [8]. Since the displacement field of a surface resonance penetrate substantially into the bulk, the calculation has been performed for a slab of 17 atomic layers, rather than for a few surface layers artificially matched to an inner set of bulk layers. The latter procedure has been largely used in previous *ab-initio* calculations [7] in order to have a sufficient statistics in the surface-projected densities of phonon states. However such matching procedure requires the rotational invariance (RI) of the dynamical matrix to be restored through the addition of artificial non-diagonal force constants [9]. The violation of the RI condition at layers where the L-resonance amplitude in not negligible may pose some problem. This difficulty is avoided in the present pure slab calculation and the results are quite

satisfactory. This calculation confirms the intrinsic nature of the surface L resonance and the previous analysis based on density-response pseudopotential [10, 11, 12] and semi-empirical Born-von-Kàrmàn [10, 11] calculations for the low-index surfaces of aluminum. The calculation also reveals the existence of new subsurface optical modes, localized in the second layer. Since these modes are not predicted by force constant models with no change in the interlayer force constants [13], they are likely to be induced by the change in the interlayer spacings near the surface. These modes, similarly to the Lucas modes in ionic crystals, form a degenerate pair at the zone center.

2. DFPT calculations and results for Al(001)

The dynamical properties of Al(001) surface were calculated by applying *first-principles* Density functional perturbation theory (DFPT) [8, 14] with ultrasoft pseudo-potential [15] and general gradient approximation (GGA-PBE) [16] for the exchange and correlation energy functional. The electron wave functions were expanded in plane waves with an energy cutoff of 25 Ry and a cutoff of 525 Ry for the charge density. The irreducible Brillouin zone was sampled over a Monkhorst-Pack grid of 10×10, resulting in 21 **k**-points. Brillouin zone integration are performed with the *smearing* technique [17], with a smearing width of $\sigma = 50$ mRy. The theoretical bulk value for the in-plane lattice constant of $a_0 = 7.62$ a.u. was used. Starting from an ideal surface the relaxation is performed by minimizing the total energy with respect to the atomic positions in the slab. At equilibrium the forces acting on the atoms are less than 0.26 meV/Å.

The relaxation of the interlayer spacing for the first four surface layers calculated in this work for two different slab thicknesses are given in Table 1 and compared with a previous DFT calculation for 7 [18, 19], 9 and 15 layers [19], with recent calculations based on the full-potential linearized augmented plane wave (FLAPW) method [20] and with the available LEED experimental data [21, 22]. The dependence on the slab thickness shows in all cases an oscillatory convergence to the thick-slab limit. The first interlayer spacing Δd_{12} calculated in this work agrees with the FLAPW result, whereas the relaxations between inner planes are found to be substantially larger than the FLAPW ones and all positive. It is noted however that the present results are in a good agreement with the LEED data, though the latter are affected by a large experimental error and are only available for the first two spacings.

The phonons are calculated for a fully relaxed Al(001) surface using 17 atomic layers in the slab and correspondingly eight atomic layers of vacuum. The dynamical matrices of the seventeen layer slab are evaluated on a 4×4 mesh of **q** points in the surface Brillouin zone. A Fourier transform of these matrices provides the real-space inter-atomic force constants of the slab layers and five neighboring atoms within the layers. The phonon dispersion curves of Al(001) calculated with DFPT for a 17 layer slab are shown in Fig. 1(a) together with the HAS experimental data reported by Gaspar *et. al.* [23]. A few more data points obtained with EELS by Mohamed and Kesmodel [24] along the Rayleigh wave dispersion curve (S_1) also in the $\bar{\Gamma}$-$\bar{\mathrm{M}}$ direction are perfectly

Table 1. The elastic relaxation of the first four surface interlayer spacings calculated in this work for Al(001) slabs of four different thicknesses (expressed in the number of layers (ML)). Comparison is made with a previous DFT calculation for 7 layers [19], a *first-principle* calculation based on full-potential linearized augmented plane wave (FLAPW) method [20] and LEED experimental data [21, 22].

Al(001)	Δd_{12} (%)	Δd_{23} (%)	Δd_{34} (%)	Δd_{45} (%)	Reference
7 ML	2.11	1.14	1.01	-	Ref. [18, 19]
9 ML	1.93	1.40	0.87	1.06	Ref. [19]
15 ML	1.41	1.13	0.83	0.60	Ref. [19]
17 ML	1.65	2.30	0.86	0.40	This work
23 ML	1.65	2.30	0.86	0.40	This work
FLAPW (9ML)	1.54	0.43	-0.02	-0.89	Ref. [20]
FLAPW (15ML)	1.60	0.55	0.02	-0.43	Ref. [20]
FLAPW (17ML)	1.60	0.44	-0.02	-0.68	Ref. [20]
LEED	1.84	2.04	-	-	Ref. [21]
LEED	2.0±0.8	1.2±0.7	-	-	Ref. [22]

superimposed to the HAS data and are not shown for clarity [26]. The agreement of the calculated S_1 dispersion curve with the HAS data is perfect. In addition to the S_1 mode, HAS data show a set of points at larger energies inside the bulk continuum which have been assigned, on basis of an *ab-initio* density response calculation [23], to two distinct branches: the upper one (labeled by S_2) is attributed to a longitudinal mode, whereas the one at lower energy (S_3) has prevalent shear-vertical character and a weaker intensity. Both surface modes fall in continuum of the bulk phonon density and are therefore to be regarded as resonances. In order to show the evolution of the slab modes into genuine surface modes the calculation for 17-layer slab is compared to a previous DFPT calculation [18] for a 7-layer slab (Fig. 1(b)). It is important to stress that also for the 17-layer slab the full dynamical matrix has been generated without insertion of bulk layers into a thinner slab with a matching of the force constants. Rotational invariance conditions are preserved, which allows to reproduce with good accuracy the experimental velocity of the Rayleigh wave.

In order to investigate the nature of the two resonances, notably of the controversial longitudinal surface resonance, the spectral intensities of the surface modes, projected onto both the first and second surface layer, have been calculated for shear-vertical (SV_1 and SV_2, respectively), longitudinal (L_1, L_2) and shear-horizontal (SH_1, SH_2) components. Their contour plots are mapped in a color scale, increasing from gray, then red to violet, on top of the dispersion curves (Fig. 2 - 4). Figure 2 shows that the SV components contribute the most, as expected, to the Rayleigh wave (S_1). The decrease in the second-layer contribution (SV_2) towards the zone boundaries reflects the decreasing penetration for increasing wavevectors. This is compensated by the second SV mode S_3 (actually a resonance) which has a large amplitude in the second layer and near the zone boundaries, whereas it only shows a weak intensity in the first layer at

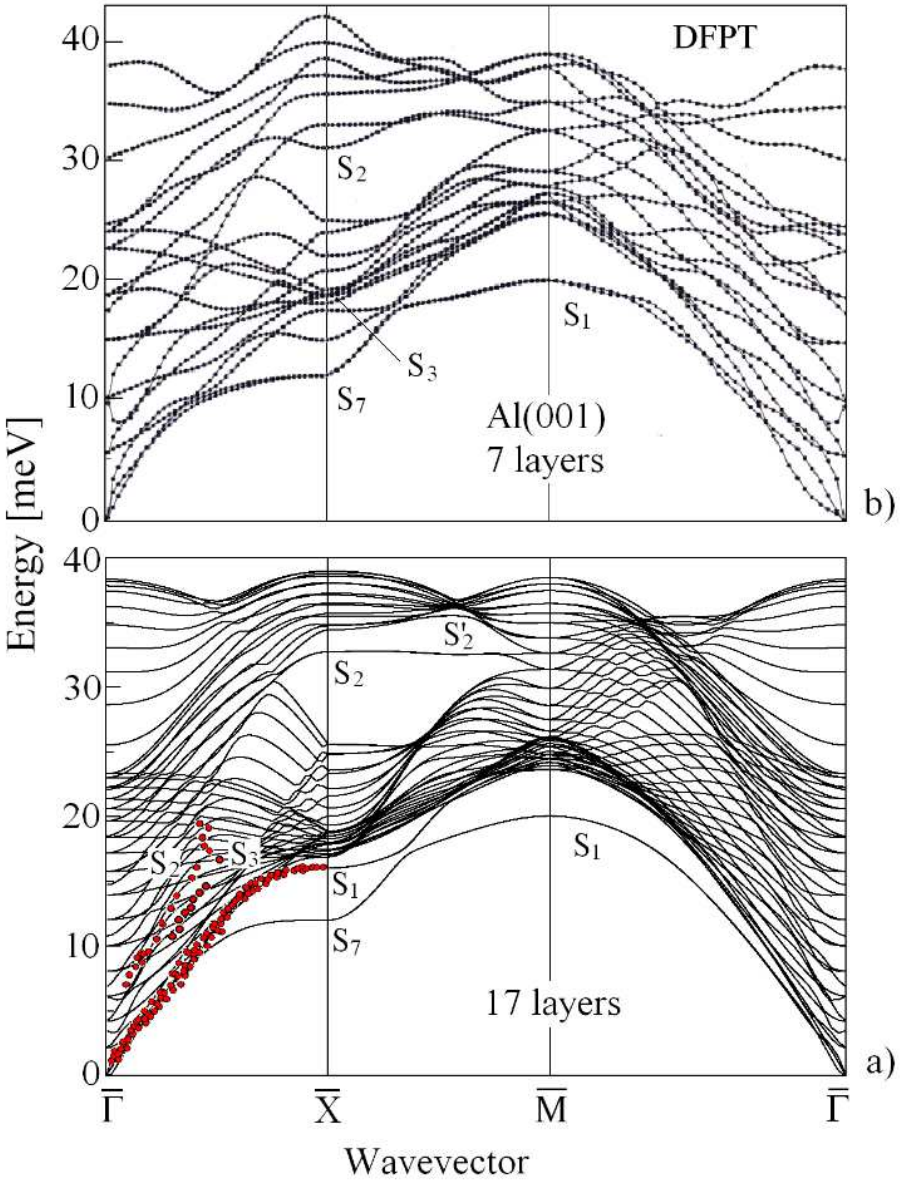

Figure 1. (a) DFPT calculated surface phonon dispersion curves for a 17-layer slab of Al(001). The experimental points corresponding to the Rayleigh wave (S_1) and to two upper branches (S_2 and S_3) have been measured by Gaspar *et. al.* with HAS spectroscopy [23]; (b) a comparison is made with a previous DFPT calculation for a 7-layer slab [19].

intermediate wavevectors, as actually observed in HAS experiments.

The longitudinal components (Fig. 3) clearly shows a large intensity just below the LA bulk edge in the first layer (L_1), terminating, along $\bar{\Gamma}$-$\bar{\mathrm{X}}$ direction, in the gap mode S_2 at $\bar{\mathrm{X}}$. In the $\bar{\Gamma}$-$\bar{\mathrm{M}}$ direction Al(001) exhibits a complex situation which deserves further experimental investigation. The S_2 resonance undergoes a considerable softening with respect to the LA edge, ending at about 26 meV at the $\bar{\mathrm{M}}$ point, just above the SV

resonance S_3 in the second layer (23 meV). In the $\bar{\Gamma}$-$\bar{\mathrm{M}}$ direction towards $\bar{\Gamma}$ the latter resonance converts into an enhancement of both the longitudinal components L_1 and L_2 near the TA band edge. On the other hand the gap mode S_2, which is longitudinal in the first layer, acquires a SV character in the second layer, whereas most of the zone-boundary longitudinal amplitude in the second layer is concentrated in the high-energy mode S_2' slightly above S_2.

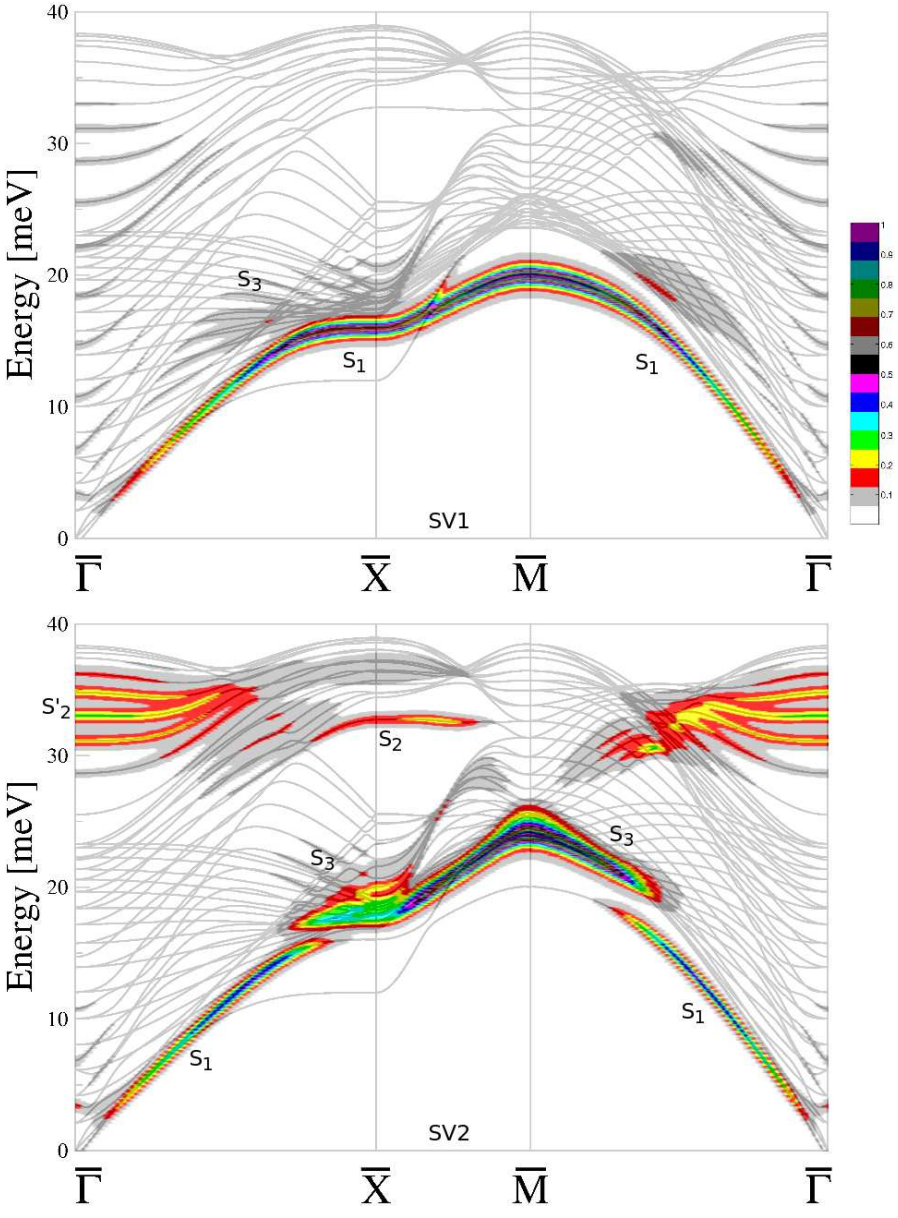

Figure 2. Contour plots of the spectral intensities of the shear-vertical components of the surface modes and resonances of Al(001) projected onto the first (SV_1) and second (SV_2) surface layer. The DFPT calculation has been performed for a 17-layer slab. The width of the S_2' resonance (present in the lower figure to the left) is larger than the separation of the bulk dispersion curves and appears to be spread over several bulk lines.

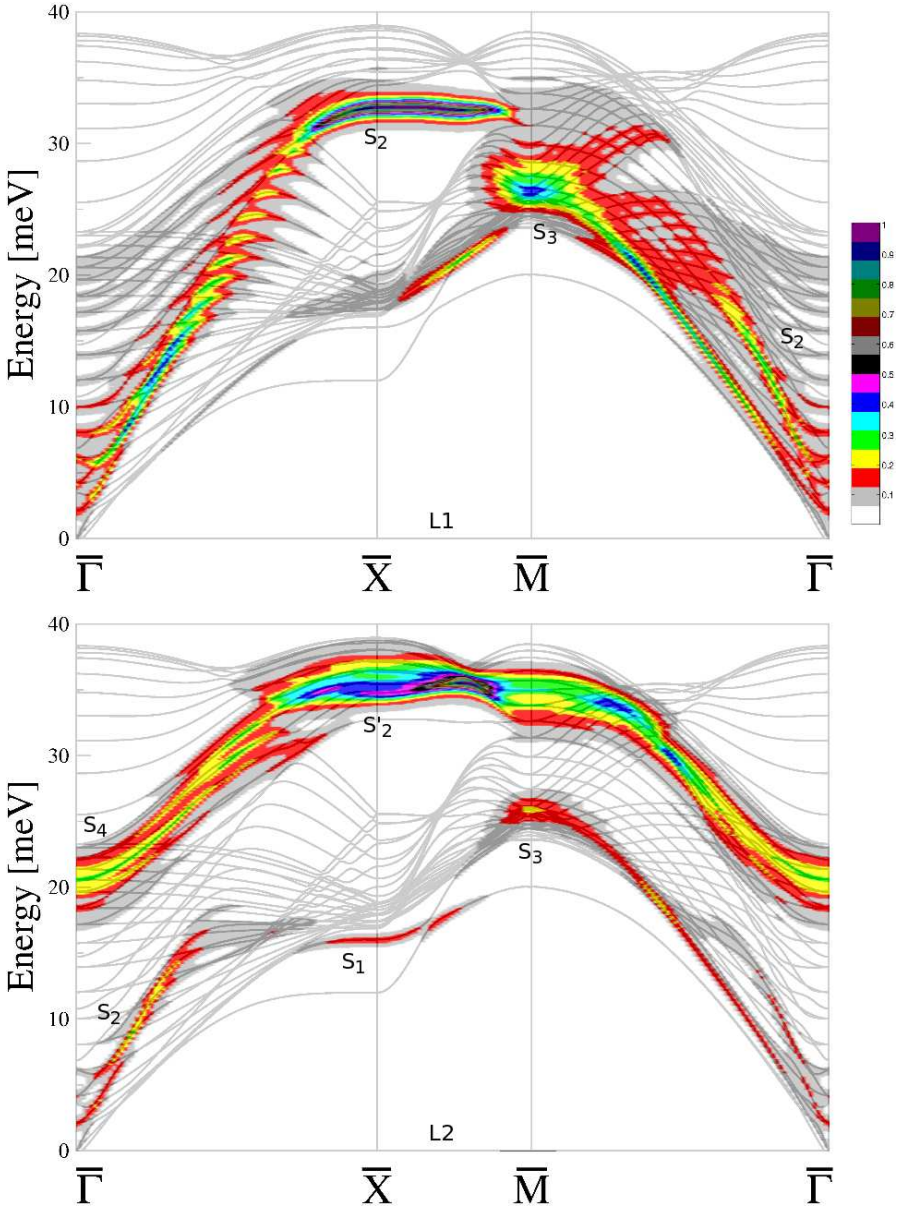

Figure 3. Same as Fig. 2 for the longitudinal components projected onto the first (L_1) and second (L_2) surface layer.

The S_2' mode (actually a resonance except in the middle of the zone boundary $\bar{\text{X}}$-$\bar{\text{M}}$) is an example of a surface phonon whose amplitude is mostly concentrated in the second layer. Its longitudinal character at the zone boundary gradually turns into a very broad, albeit intense, resonance towards the zone center. This is due to a hybridization with a second-layer L resonance (S_4), which also has a purely optical character since its energy remains finite (20 meV) at the zone center. Since empirical models with no change of interlayer force constants do not predict subsurface modes [13], these second layer resonances may be attributed to the changes in the second and third interlayer spacing (see Table 1) and may be regarded as typical effects of the extensive charge

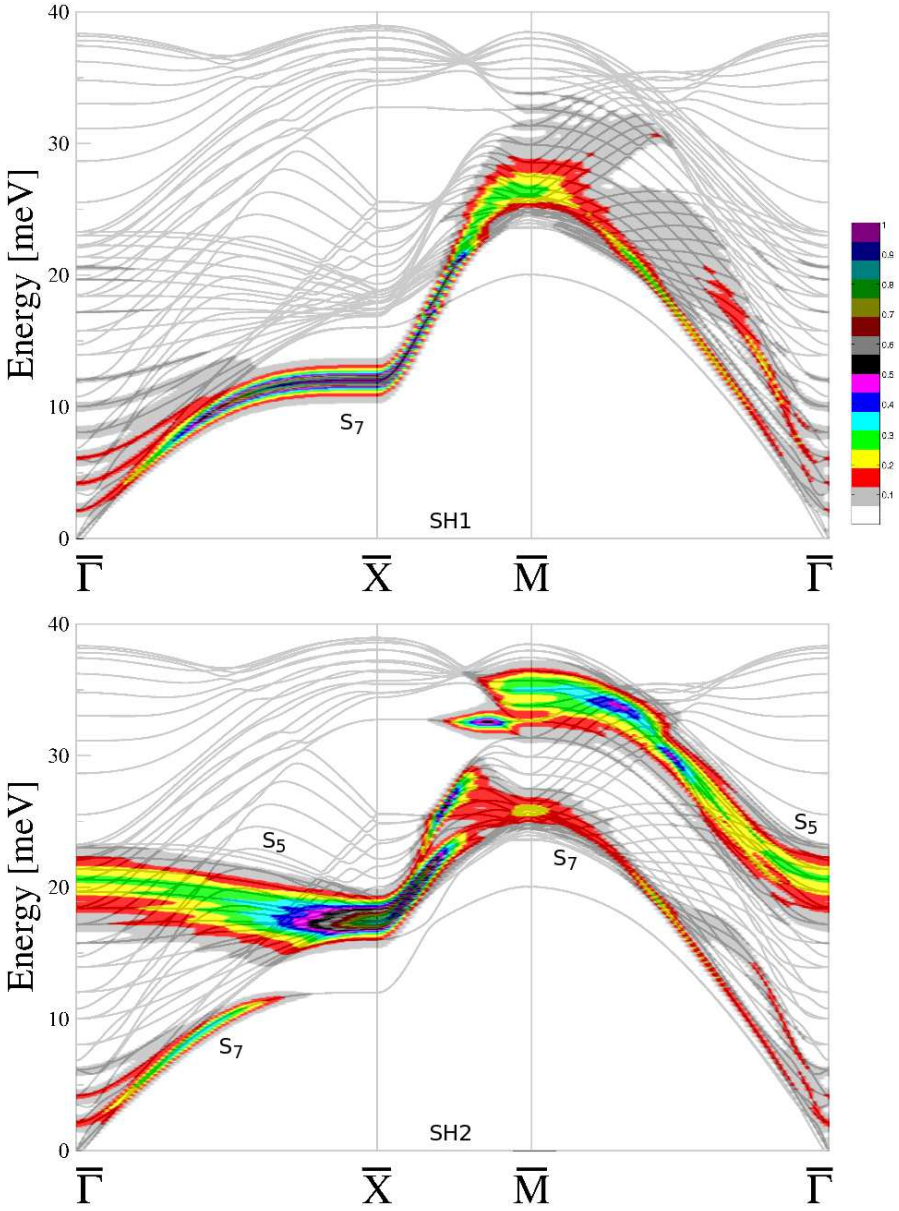

Figure 4. Same as Fig. 2 for the shear-horizontal components projected onto the first (SH_1) and second (SH_2) surface layer.

redistribution at s, p-metal surfaces.

Also the SH surface modes (Fig. 4) present an interesting structure due to the complex hybridization scheme between the acoustic SH surface mode S_7 and the second-layer optical resonance S_5, further complicated by the avoided crossing with the S_1 mode along the zone boundary $\bar{\text{X}}$-$\bar{\text{M}}$ where the sagittal plane mirror symmetry is broken. In the (001) surface of cubic crystals the acoustic SH mode S_7 is strongly localized only along the $\bar{\Gamma}$-$\bar{\text{X}}$ direction, and indeed its second-layer intensity vanishes at $\bar{\text{X}}$, whereas along $\bar{\Gamma}$-$\bar{\text{M}}$ it degenerates into the bulk band-edge SH mode. There is also a weak SH resonance occurring at long waves below the LA edge in the $\bar{\Gamma}$-$\bar{\text{M}}$ direction which is

not found in any empirical model calculations [13]. Even more interesting is the optical second-layer SH resonance S_5 which at the zone center becomes degenerate with the optical second-layer L resonance S_4. This is requested by symmetry and is reminiscent of the well-known pair of optical surface modes S_4 and S_5, discovered by Lucas [27] in cubic ionic crystals and shown to have also L and SH polarizations, respectively, and to be degenerate at $\bar{\Gamma}$ [28, 9].

The hybridization and the resulting avoided crossing of the surface modes observed with HAS spectroscopy can be better appreciated from the densities of phonon states (DOS) projected onto the sagittal (SV and L) components of the first and second surface layer along the $\bar{\Gamma}$-$\bar{\mathrm{X}}$ direction (Fig. 5). Also the experimental points (red circles) attributed to the quasi-SV and quasi-L polarizations are plotted on the respective SV_1 and L_1 density of states. As already noted in Fig. 1, the S_1 amplitude is the main feature in the SV_1 and shows the typical sine-like increase towards the $\bar{\mathrm{X}}$-point. Moreover the points at higher energy in the SV_1 correspond to a much weaker ridge arising from the small contribution of S_3 in the first layer (see Fig. 1). A similar result was found by Franchini *et. al.* in their density-response calculations [10].

As appears in Fig. 5 (L_1), the longitudinal component of S_1 is very small, indicating a small ellipticity. The main feature in L_1 is the ridge starting from the origin at $\bar{\Gamma}$ and ending into a gap mode S_2 at the $\bar{\mathrm{X}}$-point, also corresponding very well to the experimental points: this is clear confirmation that the longitudinal acoustic resonance occurs also for s,p-metal surfaces and is not just an artifact of Helium atom scattering, as speculated by Heid *et. al.* [7]. The nature of such resonance, however, is not trivial: as appears from the longitudinal amplitudes in the second layer (L_2), there is an avoided crossing between the longitudinal acoustic resonance and the surface optical branch S_4 running between 20 meV at $\bar{\Gamma}$ and 17 meV at $\bar{\mathrm{X}}$. This longitudinal optical resonance as well as the SV optical resonance occurring in the SV_2 around 34 meV have the largest amplitude on the second layer, but almost no signature on the first layer. As remarked above, this is an indication that the surface perturbation involves several layers, as correctly argued in the original analysis by Gaspar *et. al.* [23] and Franchini, Bortolani *et. al.* [10, 11]. The nature of such an extended perturbation is likely to rely all in the oscillating, slowly decaying relaxation field, which, according to the results listed in Table 1, affects a considerable number of surface layers.

A careful theoretical analysis of the dynamics of aluminum low-index surfaces was carried out by Irvine and Modena groups in which the results of semi-empirical Born-von-Kàrmàn calculations were compared to those of perturbative and non-perturbative pseudopotential density-response theories [10, 11]. An important conclusion was that the longitudinal resonance in aluminum is not related to a softening of a single force constant, as originally argued for the closed-packed nobel metal surfaces [25, 29, 30, 31], but is rather due to the cumulative effect of changes in the entire force constant field extending over several layers in the vicinity of the surface. This can be interpreted as indicating that the major changes occur in the global coupling mediated by conduction electrons.

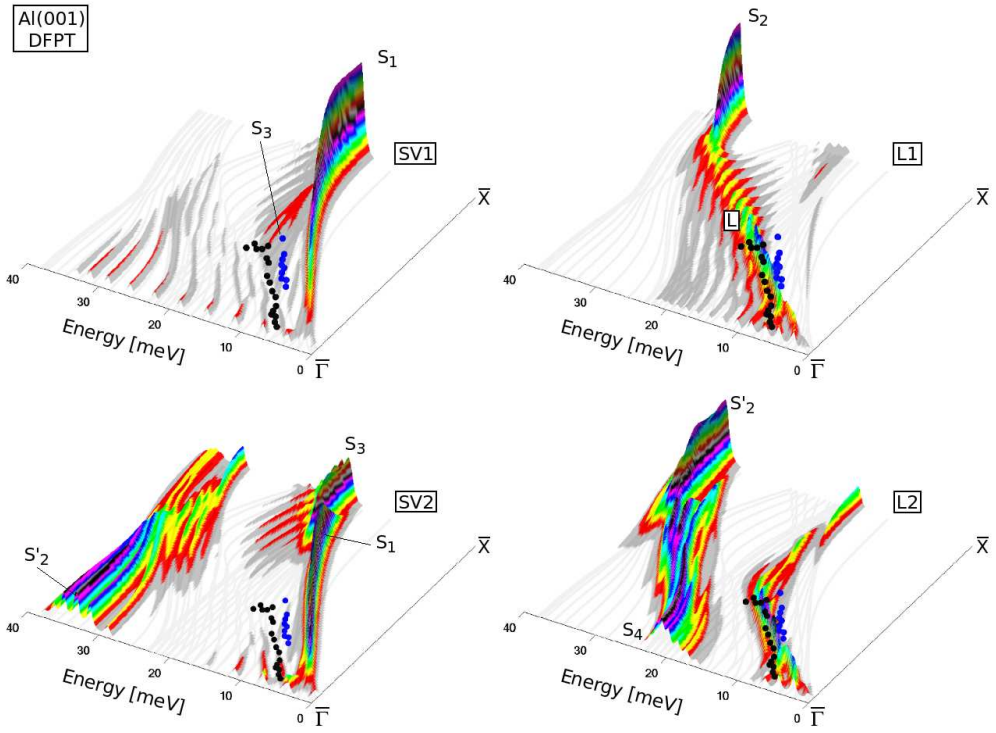

Figure 5. Comparison of HAS experimental data (black and blue circles) [23] with calculated phonon density of states projected onto the first- and second surface layer for shear-vertical (SV) and longitudinal (L) polarizations along $\bar{\Gamma}$-$\bar{\mathrm{X}}$ direction. The main features of the first-layer densities of states are the Rayleigh wave (S_1) and the acoustic L resonance, whereas the second layer densities (SV_2, L_2) show two surface optical resonances of SV and L polarization and a complex hybridization (avoided-crossing) pattern with the surface acoustic modes. The data points are plotted onto the energy-wavevector plane. N.B. the same colour scale as in previous figures.

The present DFPT calculation strongly confirms that analysis and reveals another important consequence: the existence of surface optical modes localized in the second layer of metals. They show a surprising, albeit qualitative, similarity to the microscopic surface optical modes of alkali halides, the S_4 and S_5 resonances corresponding to the Lucas mode pair arising from the TO bulk bands and the S_2' resonance being the analog of the Wallis mode associated with the LO bulk band. The typical oscillatory charge redistribution of metals may provide some hint for this analogy. It is a fact that such a dynamical structure with optical surface modes on the second layer is also found in a DFPT calculation for Cu(111), as it will be shown in a forthcoming paper [32].

Acknowledgments

Two of us (GB and JPT) acknowledge a quarter of a century of collaboration and intense discussion with Prof. Virginio (Bibi) Bortolani and his Modena group, which have triggered so much progress in the theory of surface dynamics and of the surface

phonon spectroscopy. VC acknowledges a EU Marie Curie grant N° HPMT-CT-2001-00242. Computer resources for the project have been provided by the Swedish National Infrastructure for Computing (SNIC). GB and JPT acknowledge the Alexander von Humboldt foundation for support in the framework of the AvHre-invitation program.

References

[1] A. Zangwill, Physics at Surfaces, Cambridge University Press, Cambridge 1988.
[2] H. Luth, Solid Surfaces, Interfaces and Thin Films, Springer, Heidelberg 1991.
[3] R.B. Doak, U. Harten, and J.P. Toennies, Phys. Rev. Lett. **51**, 578 (1983).
[4] U. Harten, J.P. Toennies and Ch. Wöll, Faraday Disc. Chem. Soc. **80**, 137 (1985).
[5] M. Rocca, Landolt-Bornstein, Vol. III/42 (2001).
[6] G. Armand, Solid St. Comm. **48**, 261 (1983).
[7] R. Heid and K.-P. Bohnen, Physics Reports **387**, 151 (2003).
[8] S. Baroni, S. de Gironcoli, A. Dal Corso, and P. Giannozzi, Rev. Mod. Phys. **73**, 515 (2001).
[9] G. Benedek, and J.P. Toennies, Helium Atom Scattering Spectroscopy of Surface Phonons, (Springer, Heidelberg 2007), Chap. 3 (in press).
[10] A. Franchini, V. Bortolani, G. Santoro, V. Celli, A.G. Eguiluz, J.A. Gaspar, M. Gester, A. Lock, and J.P. Toennies, Phys. Rev. B **47**, 4691 (1993).
[11] R.F. Wallis, A.A. Maradudin, V. Bortolani, A.G. Eguiluz, A.A. Quong, A. Franchini and G. Santoro, Phys. Rev. B **48**, 6043 (1993).
[12] A.E. Eguiluz and A.A. Quong, in: *Dynamical Properties of Solids*, Vol. **7**, Eds. G.K. Horton and A.A. Maradudin (North-Holland, Amsterdam 1995).
[13] J.E. Black, in: *Dynamical Properties of Solids*, Eds. by G.K. Horton, and A.A. Maradudin, Vol. 6 (Elsevier, Amsterdam 1990) p. 179.
[14] http://www.quantum-espresso.org/
[15] D. Vanderbilt, Phys. Rev. B **41**, 7892 (1990).
[16] J.P. Perdew, K. Burke, and M. Ernzerhof, Phys. Rev. Lett. **77**, 3865 (1996).
[17] M. Methfessel, and A.T. Paxton, Phys. Rev. B **40**, 3616 (1989).
[18] V. Chis, First Principles Calculations of Phonons at a Metal Surface, Växjö University Report Nr. 5 (2003).
[19] V. Chis, and B. Hellsing, Phys. Rev. Lett. **93**, 226103 (2004).
[20] J.L.F. da Silva, Phys. Rev. B **71**, 195416 (2005).
[21] W. Berndt, D. Weick, C. Stampfl, A.M. Brashaw, and M. Scheffler, Surf. Sci. **330**, 182 (1995).
[22] J.H. Petersen, A. Mikkelsen, M.M. Nielsen, and D.L. Adams, Phys. Rev. B **60**, 5963 (1999).
[23] J.A. Gaspar, A.G. Eguiluz, M. Gester, A. Lock, and J.P. Toennies, Phys. Rev. Lett. **66**, 337 (1991).
[24] M.H. Mohamed, and L.L. Kesmodel, Phys. Rev. B **37**, 6519 (1988).
[25] V. Bortolani, G. Santoro, U. Harten, and J.P. Toennies, Surf. Sci. **148**, 82 (1984).
[26] Surface modes are labelled, as it should always be, according to their polarization. Thus S_1 labels the Rayleigh mode also in the $\bar{\Gamma}$-$\bar{\mathrm{X}}$ direction. In this direction (and for this particular surface) the lowest mode frequency corresponds to a shear-horizontal mode and is therefore labelled S_7.
[27] A.A. Lucas, J. Chem. Phys. **48**, 3156 (1968).
[28] G. Benedek, and L. Miglio, in: *Surface Phonons*, Eds. F.W. de Wette and W. Kress, (Springer, Heidelberg 1991) p. 37.
[29] G. Santoro, A. Franchini, V. Bortolani, U. Harten, J.P. Toennies, and Ch. Wöll, Surf. Sci. **183**, 180 (1987).
[30] V. Bortolani, A. Franchini, F. Nizzoli, and G. Santoro, Phys. Rev. Lett. **52**, 429 (1984)
[31] V. Bortolani, A. Franchini, and G. Santoro, in Electronic, Dynamic Quantum Structural Properties of Condensed Matter, ed. by J.T. Devreese and P.E. van Camp (Plenum, New York 1985) p. 401.

[32] V. Chis, B. Hellsing, G. Benedek, M. Bernasconi, and J.P. Toennies, (to be published).